



HAL
open science

Egg provisioning explains the penetrance of symbiont-mediated sex allocation distortion in haplodiploids

Nicky Wybouw, Emma van Reempts, Jens Zarka, Flore Zélé, Dries Bonte

► **To cite this version:**

Nicky Wybouw, Emma van Reempts, Jens Zarka, Flore Zélé, Dries Bonte. Egg provisioning explains the penetrance of symbiont-mediated sex allocation distortion in haplodiploids. *Heredity*, 2023, 131 (3), pp.221-229. 10.1038/s41437-023-00638-1 . hal-04288905

HAL Id: hal-04288905

<https://hal.science/hal-04288905>

Submitted on 16 Nov 2023

HAL is a multi-disciplinary open access archive for the deposit and dissemination of scientific research documents, whether they are published or not. The documents may come from teaching and research institutions in France or abroad, or from public or private research centers.

L'archive ouverte pluridisciplinaire **HAL**, est destinée au dépôt et à la diffusion de documents scientifiques de niveau recherche, publiés ou non, émanant des établissements d'enseignement et de recherche français ou étrangers, des laboratoires publics ou privés.

Egg provisioning explains the penetrance of symbiont-mediated sex allocation distortion in haplodiploids

Nicky Wybouw¹, Emma Van Reempts¹, Jens Zarka¹, Flore Zélé² and Dries Bonte¹

¹ Terrestrial Ecology Unit, Department of Biology, Faculty of Sciences, Ghent University, Ghent, Belgium

² Institute of Evolutionary Science (ISEM), University of Montpellier, CNRS, IRD, EPHE, Montpellier 34095, France

Abstract

Maternally transmitted symbionts such as *Wolbachia* can alter sex allocation in haplodiploid arthropods. By biasing population sex ratios towards females, these changes in sex allocation may facilitate the spread of symbionts. In contrast to symbiont-induced cytoplasmic incompatibility (CI), the mechanisms that underpin sex allocation distortion remain poorly understood. Using a nuclear genotype reference panel of the haplodiploid mite *Tetranychus urticae* and a single *Wolbachia* variant that is able to simultaneously induce sex allocation distortion and CI, we unraveled the mechanistic basis of *Wolbachia*-mediated sex allocation distortion. Host genotype was an important determinant for the strength of sex allocation distortion. We further show that sex allocation distortion by *Wolbachia* in haplodiploid mites is driven by increasing egg size, hereby promoting egg fertilization. This change in reproductive physiology was also coupled to increased male and female adult size. Our results echo previous work on *Cardinium* symbionts, suggesting that sex allocation distortion by regulating host investment in egg size is a common strategy among symbionts that infect haplodiploids. To better understand the relevance that sex allocation distortion may have for the spread of *Wolbachia* in natural haplodiploid populations, we parametrized a model based on generated phenotypic data. Our simulations show that empirically derived levels of sex allocation distortion can be sufficient to remove invasion thresholds, allowing CI to drive the spread of *Wolbachia* independently of the initial infection frequency. Our findings help elucidate the mechanisms that underlie the widespread occurrence of symbionts in haplodiploid arthropods and the evolution of sex allocation.

Introduction

Maternally inherited symbionts can spread rapidly within arthropod populations by inducing a variety of reproductive phenotypes in their host (Engelstädter and Hurst, 2009). These reproductive phenotypes increase the proportion of infected females that transmit the symbiont in host populations. Cytoplasmic incompatibility (CI) is currently recognized as the most common reproductive manipulation. CI interferes with the development of uninfected host embryos that were fertilized by infected males (Beckmann *et al.*, 2019; Shropshire *et al.*, 2020). In arthropod hosts with a haplodiploid mode of reproduction (unfertilized eggs develop into haploid males and fertilized eggs into diploid females), fertilized eggs that suffer from symbiont-induced CI have two developmental outcomes. Embryos either die before reaching adulthood (Female Mortality CI (FM-CI)) or develop into viable males (Male Development CI (MD-CI)) (Vavre *et al.*, 2001; Perrot-Minnot *et al.*, 2002) (Figure 1). Previous work showed that a single CI cross in haplodiploids can simultaneously result in FM-CI and MD-CI (Vavre *et al.*, 2001; Wybouw *et al.*, 2022) (Figure 1). As CI is rescued when males and females have an identical infection state, the reproductive phenotype provides a selective advantage to transmitting females. In haplodiploid arthropods, parthenogenesis induction is another classic and well-studied invasion strategy of symbionts (Ma and Schwander, 2017). In contrast to CI, symbiont-induced parthenogenesis does not rely on egg fertilization and causes a diploidization of unfertilized eggs, generating parthenogenetic females instead of males that do not transmit

48 the symbiont (Weeks and Breeuwer, 2001; Ma and Schwander, 2017). Another, much less
49 understood, strategy of maternally transmitted symbionts to increase the proportion of infected
50 females in haplodiploid host populations consists of directly altering sex allocation (i.e. the
51 parental investment of resources to female vs. male offspring).

52 As for CI, egg fertilization by males is essential for sex allocation distortion. However,
53 in contrast to CI, sex allocation distortion occurs in crosses with infected females and is not
54 contingent on the infection state of males (Figure 1). These changes in sex allocation result in
55 female-biased broods of infected females compared to those of uninfected females. To our
56 knowledge, this reproductive phenotype was first described in a strain of the haplodiploid
57 spider mite *Tetranychus urticae* that was infected with *Wolbachia* (Vala *et al.*, 2000, 2003). In
58 addition to *Wolbachia*, sex allocation distortion is now associated with other bacterial
59 symbionts. *Rickettsia*, *Hamiltonella*, and *Arsenophonus* influence offspring sex ratio of infected
60 females in haplodiploid whitefly species (Himler *et al.*, 2011; Shan *et al.*, 2019; Wang *et al.*,
61 2020). Similarly, *Cardinium* also influence sex allocation in infected Kelly's citrus thrips
62 *Pezothrips kellyanus* in favour of female offspring (Katlav *et al.*, 2022). Haplodiploid
63 arthropods, including *Tetranychus* mites and *Pezothrips* insects, allocate egg fertilization and
64 female development to larger eggs (Macke *et al.*, 2011; Katlav, Cook, *et al.*, 2021). Katlav *et al.*,
65 2022 show that *Cardinium* affect sex allocation in *P. kellyanus* by increasing egg size
66 investment, hereby facilitating egg fertilization (and thus female development). *Cardinium*-
67 mediated increase in egg size also led to progeny that were characterized by a higher survival
68 rate and larger adult body size. In contrast, we do not understand how *Wolbachia* induce sex
69 allocation distortion. The host genotype modulates the expression of many *Wolbachia*-induced
70 reproductive phenotypes (Fujii *et al.*, 2001; Kaur *et al.*, 2021; Wybouw *et al.*, 2022), raising the
71 question whether sex allocation distortion is also contingent on host genetics.

72 Unravelling the mechanistic underpinnings of *Wolbachia*-induced sex allocation
73 distortion is not only crucial for our fundamental understanding of host-*Wolbachia* interactions
74 but also for the development of integrated pest management that relies on *Wolbachia*. A
75 number of pest management programs take advantage of the CI drive system of *Wolbachia* to
76 replace native pest populations with *Wolbachia*-infected populations that carry favourable
77 traits, such as reduced virus transmission (Ross *et al.*, 2019). However, CI strength can be
78 weakened by varying population and environmental effects (Ross *et al.*, 2017; Wybouw *et al.*,
79 2022), threatening a collapse of the pest control technique. Previous theoretical work predicts
80 that sex allocation distortion could reinforce the effect of CI and promote the invasion of
81 *Wolbachia* from low initial infection frequencies (Egas *et al.*, 2002). Yet, the actual contribution
82 of sex allocation distortion to the spread of *Wolbachia* in natural pest populations remains
83 unclear. Indeed, this previous model was not parametrized using empirical data of *Wolbachia*
84 variants that cause both CI and sex allocation distortion. Moreover, in conflict with recent
85 findings (Wybouw *et al.*, 2022), the previous model did not allow for a simultaneous expression
86 of FM-CI and MD-CI in single CI crosses. Understanding whether and how sex allocation of
87 haplodiploid pests can be altered during population replacement events is critical to predict the
88 outcome of *Wolbachia*-based pest control.

89 Here, we use the haplodiploid *Tetranychus* system to study a *Wolbachia* variant that
90 simultaneously induces CI and sex allocation distortion. We show that sex allocation distortion
91 is determined by the host background using a nuclear genotype reference panel of *T. urticae*.
92 We further examined whether this reproductive phenotype is associated with changes in
93 oviposition and immature survival rate. We tested whether, in analogy with *Cardinium*,
94 *Wolbachia* also control sex allocation of haplodiploid hosts via egg size provisioning, and
95 whether sex allocation distortion is associated with changes in adult size. Our results reveal
96 signatures of convergent mechanisms of sex allocation distortion across two divergent host-

97 symbiont systems. Finally, we parametrized a mathematical model to determine whether our
98 observed levels of sex allocation distortion would contribute to the invasion of *Wolbachia* in
99 natural haplodiploid populations.

100

101 **Materials and methods**

102 **Mite lines and maintenance**

103 We selected six *T. urticae* near-isogenic lines from the nuclear genotype reference panel
104 described in Wybouw *et al.*, 2022; Beis-*w*, Beis-*c*, LonX-*w*, LonX-*c*, Stt-*w*, and Stt-*c*. These
105 lines are composed of three different near-isogenic nuclear genotypes (Beis, LonX, and Stt)
106 that were transferred by seven rounds of iterative paternal introgression into a single cytoplasm
107 that was originally recovered from the *Wolbachia*-infected Scp-*w* line. All lines share a single
108 mitochondrion and were either infected with a single CI-inducing *Wolbachia* variant (indicated
109 by “-*w*”) or were cured of the infection by antibiotic treatment (indicated by “-*c*”) (Wybouw *et*
110 *al.*, 2022). After antibiotic curing, the cured lines were propagated for ~18 generations before
111 the onset of the experiments. Selection of the three nuclear genotypes from the reference
112 panel was based on CI strength and phenotype. In addition, we also used the original Stt near-
113 isogenic line that was naturally uninfected and did not undergo any antibiotic treatment.
114 Infection states of *Wolbachia* and other maternally transmitted symbionts were confirmed
115 before the start of the experiments by diagnostic PCR assays, as previously described
116 (Wybouw *et al.*, 2022). Mite lines were propagated by serial passage on detached bean leaves
117 (*Phaseolus vulgaris* L. cv ‘Prelude’) at 24°C, 60% RH, and a 16:8 light:dark photoperiod.

118 **Effects of *Wolbachia* on sex allocation**

119 To obtain estimates of sex ratio and immature stage survival (ISS), we generated age cohorts
120 of the mite lines by allowing 75 randomly collected adult females to oviposit for 24 hours on a
121 detached bean leaf. At the end of offspring development (between nine and eleven days post-
122 oviposition), ~50 females were isolated on a single day as teleiochrysalids (the last immobile
123 molting stage before reaching adulthood). These females were paired with ~30 one- to three-
124 day old adult males of their own line on a detached bean leaf, allowing for compatible within-
125 line matings. Three days were given to the females to emerge as virgin adults, and for matings
126 to occur (we confirmed that the near-isogenic lines exhibit high copulation propensity under
127 laboratory conditions; Supplementary information Box S1). Replicates were established by
128 pooling five females (males were discarded) and allowing oviposition on 16 cm² leaf discs for
129 three days. Females were removed from the leaf discs and eggs were counted. Male and
130 female offspring were collected and counted upon reaching adulthood. For Beis-*w*, Beis-*c*,
131 LonX-*w*, LonX-*c*, Stt-*w*, and Stt-*c*, a total of 14 replicates were performed per line across three
132 different batches (experimental blocks, each corresponding to a different age cohort). To fully
133 ensure that the observed decrease in sex ratio in Stt-*c* vs. Stt-*w* was not associated with long-
134 term deleterious effects of the antibiotic treatment, we expanded the experimental set-up for
135 this host genotype by adding the original uninfected near-isogenic Stt line. Here, following the
136 same rearing and mating protocol as described above, five replicates for Stt (uninfected), Stt-
137 *w* (infected), and Stt-*c* (cured) were performed in a single batch.

138 To verify that the effect of *Wolbachia* on the sex ratio of Stt-*w* is not caused by
139 *Wolbachia*-mediated parthenogenesis, feminization, or male killing, we isolated ~50
140 teleiochrysalid females from age cohorts of Stt-*c* and Stt-*w* as described above. We allowed
141 the teleiochrysalids to hatch into virgin adult females and feed on a detached bean leaf for
142 three days. As above, replicates were established by pooling five females on 16 cm² leaf discs
143 and allowing oviposition for three days. Females were removed from the leaf discs and eggs

144 were counted. Male and female offspring were collected and counted upon reaching
145 adulthood. For both Stt-c and Stt-w, a total of nine replicates were performed across two
146 different batches.

147

148 **Effects of *Wolbachia* on offspring number and size**

149 To obtain accurate estimates of oviposition rates, we isolated ~50 teleiochrysalid females from
150 age cohorts of Beis-w, Beis-c, LonX-w, LonX-c, Stt-w, and Stt-c, created as described above.
151 These females were paired with ~30 one- to three-day old adult males on a detached bean
152 leaf and were allowed to mate for three days. Replicates were established by pooling two
153 females and allowing oviposition on 16 cm² leaf discs for 24 hours. Two hours after creating
154 the replicates, all experimental females were examined to ensure they survived the transfer.
155 Replicates with one or two dead females were removed from further analyses. After the
156 oviposition interval, females were removed from the leaf discs and eggs were counted. The
157 number of replicates per mite line ranged between 25 and 43 and were performed across four
158 different batches.

159 To determine the effect of *Wolbachia* infection on *Tetranychus* egg size, eggs were
160 randomly sampled from the leaf discs that were used to estimate oviposition rates for Beis-w,
161 Beis-c, LonX-w, LonX-c, Stt-w, and Stt-c. Here, we focused on eggs that were oviposited
162 across three batches of the oviposition tests. Eggs were photographed under a binocular
163 microscope (6x 10x) using a Leica M50 camera (5 MP HD Microscope Camera Leica MC170
164 HD). Between 125 and 197 eggs were analyzed for each mite line (with a total of 971 eggs).
165 To confirm that sex allocation is mediated by egg size in *T. urticae* (Macke *et al.*, 2011),
166 between 21 and 37 photographed eggs from Beis-c, Beis-w, LonX-c, and LonX-w were isolated
167 and transferred to separate 4 cm² leaf discs (with a total of 124 eggs). Sex was determined at
168 the sexually dimorphic teleiochrysalid stage. Photos were analyzed using *Natsumushi* image
169 measuring software (Tanahashi and Fukatsu, 2018). For each egg, *Natsumushi* generated a
170 smoothed outline based on eight manually specified demarcating points and automatically
171 extracted the projected egg area. The total egg surface was calculated by assuming a spherical
172 shape, following previous studies (Macke *et al.*, 2011, 2012).

173 To determine the effect of *Wolbachia* infection on *Tetranychus* adult size, ~75 adult
174 females were isolated from age cohorts of LonX-w, LonX-c, Stt-w, and Stt-c, and allowed to
175 oviposit on a detached bean leaf for 24 hours. Larval offspring were collected upon hatching
176 and 12 larvae were pooled on 16 cm² leaf discs to ensure equal population densities. As adult
177 mites are highly mobile and are difficult to position in equal planes, we used the projected body
178 surface of teleiochrysalids as a proxy for adult size. Both male and female teleiochrysalids
179 were isolated, placed on a flat perspex slide, and photographed as described above. Using
180 *Natsumushi* image measuring software (Tanahashi and Fukatsu, 2018), the projected
181 teleiochrysalid surface was measured by manually specifying ten demarcating points. Between
182 55 and 66 teleiochrysalids were analyzed for each mite line. In contrast to egg size, adult size
183 was not expressed as total surface, but as the projected surface area.

184 **Statistical analyses**

185 All analyses were carried out using R (version 4.1.3) (R Core Team, 2021). Raw data and the
186 R script are publicly accessible as Supplementary Files and the statistical models are
187 described in Table S1. Sex ratio was calculated as the proportion of females among the
188 progeny that successfully reached adulthood. Immature stage survival (ISS) included
189 embryonic and juvenile survival and was defined as the proportion of adult offspring over the
190 total number of eggs. Daily oviposition was computed as the number of eggs per alive female

191 (oviposition was allowed for 24 hours only). All data, except copulation latency (Supplementary
 192 information Box S1), were analyzed using generalized linear mixed models (*glmmTMB*
 193 function of the “glmmTMB” package) (Brooks *et al.*, 2017). Proportional data, sex ratio and
 194 ISS, were examined with a Binomial (or Betabinomial to account for overdispersion) error
 195 distribution, with a logit link. Continuous data, oviposition, egg surface, male and female adult
 196 size were fitted with a Gaussian error distribution (Table S1). In the case of non-normal error
 197 distribution, the response variables were linearized using a Box-cox transformation prior to
 198 analysis (*boxcox* function of the “MASS” package was used to find the appropriate value of
 199 lambda) (Crawley, 2007). For most of the statistical models, genotype, infection state and their
 200 interaction were fit as fixed explanatory variables, whereas batch was considered as a random
 201 explanatory variable. To analyze sex ratio within the Stt background (Stt, Stt-c, and Stt-w), only
 202 the infection state was used as a fixed explanatory variable. For the analysis of female and
 203 male egg surface, offspring sex along with all two- and three-way interactions with the
 204 genotype and/or infection state were added as fixed explanatory variables. Maximal models,
 205 including all higher order interactions, were simplified by sequentially eliminating non-
 206 significant terms and interactions to establish minimal models. The significance of the
 207 explanatory variables was established using chi-square tests (*Anova* function of the “car”
 208 package). The reported significant chi-squared values are for the minimal model while the non-
 209 significant values were obtained before removing the variable from the minimal model
 210 (Crawley, 2007). When interactions or factors with more than two levels were significant,
 211 differences among levels were analyzed using multiple comparisons (*pairs* function of the
 212 “emmeans” package (Lenth *et al.*, 2022)), with Bonferroni corrections to account for multiple
 213 testing.

214 **Modelling *Wolbachia* invasion in *Tetranychus* populations**

215 To determine how sex allocation distortion, combined with varying CI phenotype (FM- and/or
 216 MD-CI) and strength, may affect the spread of a *Wolbachia* variant in divergent *Tetranychus*
 217 populations, we extended a mathematical model previously developed by Vavre *et al.*, 2000
 218 and Egas *et al.*, 2002. The proportion of females (f_t) and males (m_t) that are infected at
 219 generation t , are given by the following equations:

220

$$221 \quad f_{t+1} = \frac{f_t \cdot F \cdot ISS \cdot Sd \cdot (1 - \mu)}{f_t \cdot F \cdot ISS \cdot Sd \cdot (1 - \mu \cdot CI \cdot m_t) + (1 - f_t)(1 - CI \cdot m_t)}$$

$$222 \quad m_{t+1} = \frac{f_t \cdot F \cdot ISS \cdot (1 - \mu)(1 - k \cdot Sd)}{f_t \cdot F \cdot ISS \cdot (1 - k \cdot Sd + \mu \cdot k \cdot Sd \cdot MD \cdot m_t) + (1 - f_t)(1 - k + k \cdot MD \cdot m_t)}$$

223 where most of the parameters correspond to those in Vavre *et al.*, 2000. F is the relative
 224 fecundity of infected vs. uninfected females, ISS the relative immature stage survival of
 225 infected vs. uninfected offspring, and μ the proportion of uninfected eggs produced by infected
 226 females (transmission efficiency is thus given by $1-\mu$). k corresponds to the fertilization rate of
 227 eggs (i.e., estimated as the female to adult ratio in control crosses), and Sd to the sex allocation
 228 distortion induced by *Wolbachia* in the brood of infected females (i.e., the ratio of female to
 229 adult in the brood of infected females relative to uninfected females in control crosses).
 230 Finally, CI is the total proportion of eggs affected by CI (i.e., total CI strength), computed as a
 231 function of MD and FM , which correspond to the MD- and FM-CI phenotypes, respectively (MD
 232 and FM are equal to the corrected indexes MD_{corr} and FM_{corr} , respectively) (Poinsot *et al.*,
 233 1998; Cattel *et al.*, 2018; Zélé *et al.*, 2020; Cruz *et al.*, 2021; Wybouw *et al.*, 2022). Assuming
 234 that the effects of both CI phenotypes are independent, total CI should be computed as $CI =$
 235 $MD + FM \cdot (1 - MD)$. In the current study, however, we computed total CI as $CI = MD + FM$,

236 as the implemented FM_{corr} indexes already account for a potential decrease in female
237 production due to MD-CI (i.e. these indexes were already corrected using MD_{corr} ; Wybouw *et*
238 *al.*, 2022).

239 In this model, *Wolbachia* infection frequency in females is calculated by the same
240 formula as when only MD- or FM-CI is considered (Egas *et al.*, 2002, and Vavre *et al.*, 2000
241 for $Sd = 1$). The difference lies in how the *CI* parameter is computed. As only MD-CI directly
242 affects the proportion of infected males, the formula for *Wolbachia* infection frequency in males
243 is the same as previous models that only consider MD-CI, and when $MD = 0$, it is also the
244 same as those that only consider FM-CI (Vavre *et al.*, 2000 for $Sd = 1$). Note, however, that
245 the current formula differs from that of Egas *et al.*, 2002 for MD-CI, as one category of
246 uninfected males produced by uninfected females, is missing in the denominator of the
247 previous model. The category corresponds to uninfected eggs fertilized by the sperm of
248 infected males that develop as males instead of females due to MD-CI, given by $(1 - f_t)(k \cdot$
249 $MD \cdot m_t)$.

250 As in Egas *et al.*, 2002 and Vavre *et al.*, 2000, when *Wolbachia* induce CI, the model
251 can yield three different equilibria: (1) an unstable polymorphic equilibrium, which corresponds
252 to 'the threshold infection frequency for *Wolbachia* invasion' known in diploid species
253 (Hoffmann *et al.*, 1990; Turelli, 1994); (2) a stable polymorphic equilibrium, which is reached
254 when the initial infection frequency is above the unstable equilibrium (note that only perfectly
255 transmitted *Wolbachia* can fully invade a host population; i.e. this equilibrium can equal 1 only
256 when $\mu = 0$), and (3) an equilibrium where *Wolbachia* infection is purged, which is reached
257 when the initial infection frequency is below the unstable equilibrium. When *Wolbachia* do not
258 induce CI, only one polymorphic equilibrium can exist that is either stable or unstable when
259 *Wolbachia* are beneficial or costly for the host, respectively. Analytical solutions and main
260 equilibrial conditions are provided in the Supplementary Box S2.

261 **Results**

262 **Sex allocation in *Tetranychus* relies on an interaction between host and *Wolbachia***

263 To study *Wolbachia*-induced sex allocation distortion in *Tetranychus*, we selected three
264 nuclear genotypes, Beis, LonX, and Stt that were either infected with a single *Wolbachia*
265 variant ('-w' suffix) or cured via antibiotic treatment ('-c' suffix) (Wybouw *et al.*, 2022). Selection
266 of these nuclear genotypes was based on varying CI strength and phenotype. Whereas Beis
267 is typified by complete CI, LonX and Stt exhibit intermediate CI strength. The CI phenotype is
268 characterized by a combination of MD-CI and FM-CI in LonX, while only consisting of FM-CI
269 in Beis and Stt (Wybouw *et al.*, 2022). We performed compatible within-line crosses for these
270 *Wolbachia*-infected and cured sister lines. The interaction between nuclear genotype and the
271 *Wolbachia* infection state significantly affected the female-biased sex ratios ($\chi^2_2=14.6286$,
272 $p=0.0007$) (Figure 2). Within-genotype *a posteriori* comparisons revealed that the average sex
273 ratio increased by ~11% when Stt females were infected with *Wolbachia* (t -ratio=4.272,
274 $p=0.0005$), whereas the sex ratios were not significantly different within Beis nor LonX (t -
275 ratio=1.125, $p=1.0000$ and t -ratio=1.847, $p=0.6176$, respectively) (Figure 2 and Table S2). In
276 a second experiment, we included the naturally uninfected Stt line to rule out any potential
277 long-term interference of the antibiotic treatment on sex ratio. Infection state determined the
278 female-biased sex ratio ($\chi^2_2=18.9370$, $p<0.0001$). No significant difference was found between
279 uninfected Stt and cured Stt-c (t -ratio=0.110, $p=1.0000$), whereas the sex ratio of infected Stt-
280 w was higher to both *Wolbachia*-free lines (vs. Stt-c: t -ratio=3.964, $p=0.0056$ and vs. Stt: t -
281 ratio=3.864, $p=0.0068$) (Figure 2). Together with the non-differential sex ratios between the
282 infected and cured sister lines of the Beis and LonX genotype (Figure 2), this is strong evidence
283 that the antibiotic treatment had no long-term effects on observed sex ratios.

284 Host genotype, infection state, and their interaction did not significantly affect immature
285 stage survival (ISS). ISS is therefore not associated with the change in sex ratio within the Stt
286 background (Figure S1 and Table S3). We also investigated the offspring sex ratio and ISS of
287 virgin Stt-w and Stt-c females to test whether the *Wolbachia* variant induces parthenogenesis,
288 feminization, or male killing within the Stt background. All offspring were male, ruling out
289 *Wolbachia*-mediated parthenogenesis and feminization. As no significant difference in ISS was
290 observed between the infected and cured line ($\chi^2_1=0.0000$, $p=0.9949$), the hypothesis of
291 *Wolbachia*-induced male killing was also rejected (Figure S1 and Table S3). This further shows
292 that *Wolbachia* infection does not cause any particular survival costs in the focal nuclear
293 genotypes during offspring development. However, the interaction between host genotype and
294 the *Wolbachia* infection state significantly determined daily oviposition ($\chi^2_2=9.0006$, $p=0.0111$)
295 (Figure 3 and Table S4). Comparisons within host nuclear backgrounds uncovered that the
296 daily oviposition rates were only significantly different between the infected and cured line of
297 the LonX genotype (t -ratio=5.704, $p<0.0001$). For the LonX genotype, *Wolbachia* infection
298 decreased daily oviposition (Figure 3).

299 ***Wolbachia* control host sex allocation by regulating egg provisioning**

300 In *Tetranychus* mites, the probability of egg fertilization (and subsequent female development)
301 positively covaries with egg size (Macke *et al.*, 2011). Here, we confirm that sex allocation is
302 mediated by egg size by tracking the offspring of Beis-w, Beis-c, LonX-w, and LonX-c.
303 Statistical analyses revealed that female egg surface was significantly larger ($\chi^2_1=28.8573$,
304 $p<0.0001$), and also varied depending on the interaction between nuclear genotype and the
305 infection state ($\chi^2_3=11.1822$, $p=0.0008$) (Figure S2). In haplodiploid *Pezothrips* insects,
306 *Cardinium* manipulate sex allocation by increasing egg size, hereby facilitating egg fertilization
307 (Katlav *et al.*, 2022). We tested whether *Wolbachia* achieve higher female-biased sex ratios in
308 Stt mites by inducing similar changes in the host reproductive physiology. We quantified egg
309 size across the infected and cured lines of the three *T. urticae* genotypes and again observed
310 that the interaction between host genotype and the *Wolbachia* infection state significantly
311 affected egg surface ($\chi^2_2=97.0092$, $p<0.0001$) (Figure 4). Although we observed that *Wolbachia*
312 infection only biased the sex ratio of Stt mites, we found that for both LonX and Stt mites,
313 *Wolbachia*-infected females oviposited larger eggs compared to cured females (t -ratio=7.030,
314 $p<0.0001$ and t -ratio=12.606, $p<0.0001$, respectively). However, on average, *Wolbachia*
315 infection increased egg surface by ~11% in Stt mites and by only ~5% in LonX mites (Figure
316 4 and Table S5). In contrast, egg size was not significantly different within the Beis genotype
317 (t -ratio=0.541, $p=1.0000$).

318 Egg size positively covaries with adult size in *Tetranychus* mites (Macke *et al.*, 2011),
319 raising the question whether the *Wolbachia*-mediated increase in egg size also results in larger
320 adults for the LonX and Stt genotypes. Using the projected body surface of teleiochrysalids
321 (final molting stage before adulthood) as a proxy, our results show that the interaction between
322 host genotype and the *Wolbachia* infection state significantly affected the adult size for both
323 males and females (males: $\chi^2_1=14.5653$, $p=0.0001$ and females: $\chi^2_1=11.4769$, $p=0.0007$)
324 (Figure 5). *Wolbachia* infection significantly increased male and female adult size within the
325 Stt genotype (males: t -ratio=4.310, $p=0.0002$ and females: t -ratio=3.255, $p=0.0058$), but no
326 significant differences were observed for LonX (males: t -ratio=0.998, $p=1.0000$ and females:
327 t -ratio=1.542, $p=0.5021$) (Figure 5). For the Stt genotype, the projected body area of
328 teleiochrysalid males and females were ~10% and ~5% larger in response to *Wolbachia*
329 infection, respectively (Figure 5 and Table S6).

330

331

332 Sex allocation distortion removes the threshold for *Wolbachia* invasion

333 We predicted the spread of *Wolbachia* in the three *T. urticae* nuclear genotypes and assessed
334 the effect of sex allocation distortion on infection dynamics by adapting previously developed
335 deterministic models for haplodiploids (Vavre *et al.*, 2000; Egas *et al.*, 2002). As observed for
336 the LonX genotype, a single CI cross can lead to a mixture of FM-CI and MD-CI (Wybouw *et al.*,
337 2022), an outcome that is now incorporated into the revised version of the model (Table
338 S7 provides the full comparison between our and previous models).

339 For the Beis and LonX genotypes, simulations for *Wolbachia* invasion revealed that
340 estimated fitness costs of *Wolbachia* infection result in unstable equilibria under which infection
341 is lost after a number of host generations (i.e., the threshold infection frequency for *Wolbachia*
342 invasion) (Figure 6). In particular, the high fecundity costs estimated in LonX leads to the
343 highest threshold (~46% vs. ~16% in Beis; Figure 6). Above the threshold frequency,
344 *Wolbachia* are predicted to spread the fastest in populations of the Beis nuclear genotype, in
345 which total CI strength is the strongest (~100% in Beis, ~65% in LonX, and ~50% in Stt; Table
346 S8). In contrast, despite similar fitness costs in Stt and Beis and weaker CI strength in the
347 former, the model does not predict a threshold frequency for *Wolbachia* invasion in Stt (Figure
348 6). Additional simulations that revoke the effect of sex allocation distortion in the Stt genotype
349 further show that the absence of an infection threshold is solely due to the *Wolbachia*-induced
350 female-biased sex ratio (Figure S3). Indeed, without sex allocation distortion in the Stt
351 genotype, only an initial infection frequency above ~24% would allow for *Wolbachia* invasion
352 (Figure S3). In agreement with these results, there is no longer a threshold frequency for
353 *Wolbachia* invasion in the Beis genotype after introducing the same level of sex allocation
354 distortion as observed for Stt (Figure S3, the unstable equilibrium becomes ~0%). In contrast,
355 the introduction of sex allocation distortion in the LonX genotype has only little effect (the
356 invasion threshold decreases from ~46% to ~43%) (Figure S3). Finally, revoking CI in each of
357 the three genotypes shows that *Wolbachia* should be purged from Beis and LonX but should
358 still spread in Stt where sex allocation distortion compensates for the infection costs (Figure
359 S3). Consistent with these observations, even though the *Wolbachia* variant induces weaker
360 CI in Stt than in LonX (~50% vs. ~65% total CI strength), the infection is predicted to spread
361 above the threshold frequency faster in Stt due to sex allocation distortion (Figure 6). Our
362 model parametrization thus shows that, in some host genotypes, sex allocation distortion can
363 strengthen the effect of CI and ensure the spread of *Wolbachia* independently of the initial
364 infection frequencies. Together, these results corroborate previous theoretical predictions of
365 the functional importance of sex allocation distortion for maternally inherited symbionts in
366 haplodiploid hosts (Egas *et al.*, 2002).

367 Discussion

368 Maternally inherited symbionts commonly infect haplodiploid arthropods and spread through
369 these host populations by inducing distinct reproductive phenotypes (Weinert *et al.*, 2015; Ma
370 and Schwander, 2017; Shropshire *et al.*, 2020; Kaur *et al.*, 2021). A growing body of evidence
371 indicates that sex allocation distortion could be a widespread, previously neglected,
372 reproductive phenotype across divergent haplodiploid host - symbiont systems (Vala *et al.*,
373 2003; Wang *et al.*, 2020; Katlav *et al.*, 2022). Yet, several questions about the mechanisms
374 that underpin sex allocation distortion are still outstanding, especially for *Wolbachia*.

375 The current results on the Stt nuclear genotype confirm that *Wolbachia* can cause
376 higher female-biased sex ratios by regulating host sex allocation in *Tetranychus* mites (Vala
377 *et al.*, 2003). Here, *Wolbachia* infection increases female production by ~11%, whereas Vala
378 *et al.*, 2003 reports an increase of ~18% in the *T. urticae* C-strain. As for other symbiont-
379 mediated phenotypes, this difference in phenotypic strength can be attributed to genetic

380 variation in *Wolbachia* and/or the arthropod host (Turelli, 1994; Engelstädter and Hurst, 2009;
381 Beckmann *et al.*, 2021; Wybouw *et al.*, 2022). The *Wolbachia* variant of the current study does
382 not induce quantifiable sex allocation distortion in the Beis and LonX genotype, suggestive of
383 strong host modulation by *Tetranychus*. These findings are consistent with a previous
384 hypothesis that *T. urticae* evolves compensatory mechanisms that suppress *Wolbachia*-
385 induced sex allocation distortion (Vala *et al.*, 2003). However, this hypothesis implies that sex
386 allocation distortion is deleterious for *Tetranychus* hosts and that suppressor systems evolved
387 in the Beis and LonX genotype to counteract the reproductive manipulations induced by
388 *Wolbachia*.

389 As the focal *Wolbachia* variant also induces CI in incompatible matings (Wybouw *et al.*,
390 2022), we show that *Wolbachia* are able to simultaneously induce CI and sex allocation
391 distortion. These observations add to a growing body of literature showing that symbiont
392 genomes often carry the genetic architecture of multiple reproductive manipulations (Fujii *et*
393 *al.*, 2001; Kaur *et al.*, 2021; Katlav *et al.*, 2022). Previous work uncovered that CI strength is
394 also determined by host modulation within the *T. urticae* nuclear genotype reference panel
395 (Wybouw *et al.*, 2022). The penetrance of sex allocation distortion and CI appears uncoupled
396 across the host genotypes. The *Wolbachia* variant only causes intermediate CI in Stt and LonX
397 (~50% and ~65%, respectively), compared to complete CI in Beis (100%). We can therefore
398 speculate that the host modifier systems act independently on the two *Wolbachia*-induced
399 reproductive phenotypes. Host modulation of CI is largely manifested in infected *Tetranychus*
400 males (Wybouw *et al.*, 2022). As the reproductive physiology of haplodiploid females is a
401 strong determinant of the sex ratio of their offspring (Overmeer and Harrison, 1969; Mitchell,
402 1972; Takafuji and Ishii, 1989; Katlav, Nguyen, *et al.*, 2021) and sex allocation distortion
403 appears independent of the infection state of males, it is likely that host modulation of sex
404 allocation distortion occurs in females. Together, this further indicates that the host modifier
405 systems of haplodiploids might have sex-specific phenotypic effects.

406 In this study, we also gathered strong evidence that *Wolbachia*-induced sex allocation
407 distortion in *Tetranychus* mites is mediated by regulating egg size. For the Stt genotype,
408 *Wolbachia*-infected females oviposit larger eggs compared to the *Wolbachia*-free sister line,
409 increasing the probability of successful fertilization and female development (Macke *et al.*,
410 2011; Katlav, Cook, *et al.*, 2021). We also noted a weaker, but significant, increase in egg size
411 for the LonX genotype. Here, *Wolbachia* infection does not cause sex allocation distortion,
412 likely because the egg size effect is too weak. As egg size also varied across the three *T.*
413 *urticae* nuclear genotypes regardless of *Wolbachia* infection, our results identify egg size
414 investment as a reproductive trait that is modulated by both the host and symbiont genotype.
415 In *Tetranychus* females, a physiological trade-off controls resource allocation into egg number
416 and size (Macke *et al.*, 2012). Here, *Wolbachia* infection influences egg number within the
417 LonX nuclear background, but not within Stt. However, only a narrow 24 hour time interval of
418 the oviposition period was monitored within our experimental set-up, raising the possibility that,
419 conversely to Macke *et al.*, 2012, we missed the full trade-off effect of increased egg size on
420 total egg number. Alternatively, this trade-off may be altered if *Wolbachia* infection causes an
421 increase in available resources for ovipositing females. Many bacterial symbionts provide
422 nutrients for their invertebrate host, including *Wolbachia* (Hosokawa *et al.*, 2010; Kaur *et al.*,
423 2021). Based on dietary supplementation experiments, symbiont-mediated provisioning of B
424 vitamins is implicated in sex ratio distortion in haplodiploid whitefly species (Wang *et al.*, 2020).
425 In addition to egg size regulation, other *Wolbachia*-mediated changes in the female
426 reproductive physiology could further contribute to sex allocation distortion. To increase the
427 likelihood of successful egg fertilization, *Wolbachia* could facilitate the flow of sperm from the
428 spermatheca to the ovary and the entry of sperm cells into the ovarian cavity (Helle, 1967;
429 Helle and Sabelis, 1985). As sperm cells tend to accumulate in the dorsal region of the ovarian

430 cavity in *Tetranychus* mites, *Wolbachia* could also promote sperm-egg contact and subsequent
431 egg fertilization by causing a more even sperm distribution within the cavity (Feiertag-Koppen
432 and Pijnacker, 1982; Helle and Sabelis, 1985).

433 Previous studies in haplodiploids uncovered a positive correlation between egg size,
434 immature survival rate, and adult body size (Macke *et al.*, 2011; Katlav, Cook, *et al.*, 2021).
435 Consistent with these studies, *Cardinium*-mediated increase in egg size is shown to be linked
436 to higher juvenile survival rate and adult size in *P. kellyanus* (Katlav *et al.*, 2022). Although
437 *Wolbachia*-infected LonX-*w* and Stt-*w* females tended to have broods with higher immature
438 survival rates than cured LonX-*c* and Stt-*c* females, we could not statistically demonstrate that
439 *Wolbachia* infection positively affects this trait in these two genotypes. However, we found that
440 *Wolbachia* infection increases male and female adult size within the Stt genotype, an effect
441 that may lead to a higher reproductive success for infected adults (Li and Zhang, 2018). In
442 *Tetranychus*, competition for mates among males can be intense, resulting in aggressive
443 fighting behavior. Larger males have an advantage in these competitive interactions, and are
444 more likely to fertilize virgin females under certain conditions (Potter *et al.*, 1976; Enders,
445 1993). A higher fertilization success of *Wolbachia*-infected males may strengthen the effect of
446 CI, further driving *Wolbachia* infection frequencies through host populations. In contrast, egg
447 size difference does not persist into the adult stage in LonX mites, which is likely explained by
448 the relatively weak egg size effect of *Wolbachia* infection in this nuclear genotype.

449 In haplodiploid *Pezothrips* insects, *Cardinium* symbionts also cause host sex allocation
450 distortion (Katlav *et al.*, 2022). The common strategy within the *Wolbachia*-*Tetranychus* and
451 *Cardinium*-*Pezothrips* systems to distort sex allocation by regulating egg size raises the
452 question of whether these symbionts share the same genetic basis for sex allocation distortion
453 or evolved this reproductive phenotype independently. CI is also induced by both *Cardinium*
454 and *Wolbachia* and is manifested by remarkably similar cytological defects (Gebiola *et al.*,
455 2017). Yet, despite a nearly identical cellular phenotype, CI appears to be underpinned by
456 different genetic architectures in these intracellular bacteria (Gotoh *et al.*, 2007; Penz *et al.*,
457 2012; LePage *et al.*, 2017; Beckmann *et al.*, 2017, 2019; Shropshire *et al.*, 2020). Our results
458 suggest that convergent mechanisms also underpin sex allocation distortion across divergent
459 biological systems. To dissect the underlying mechanisms of sex allocation distortion,
460 comparative genomics and transcriptomics data sets can be leveraged, for instance, the
461 differentially expressed gene set of *T. urticae* embryos upon *Wolbachia* infection (Bing *et al.*,
462 2020).

463 Many haplodiploid arthropods, including thrips, whiteflies, and spider mites, are
464 pathogen-carrying pests that threaten agricultural crop production (Robertson and Carroll,
465 1988; Jones, 2005; Kitajima *et al.*, 2010; Navas-Castillo *et al.*, 2011). Pest control programs
466 are being developed that rely on the driving ability of artificial *Wolbachia* infections that reduce
467 pathogen transmission (Ross *et al.*, 2019; Gong *et al.*, 2020). For successful population
468 replacement, infected individuals must be released at a rate high enough to exceed threshold
469 infection frequencies (Ross *et al.*, 2019). Here, using a parametrized model, we show that sex
470 allocation distortion could facilitate the spread of *Wolbachia* within haplodiploid pest
471 populations by removing threshold infection frequencies and increasing invasion rates.
472 Therefore, this reproductive phenotype may be instrumental to increase the efficacy of pest
473 control measures. Our results underscore the importance of studying the impact and
474 underlying mechanisms of natural and artificial *Wolbachia* infections on host sex allocation.

475 **Acknowledgements**

476 We thank Masahiko Tanahashi for assisting with the *Natsumushi* analyses, Sara Magalhães
477 and Fabrice Vavre for useful discussions, Martijn Egas for confirming the error in Egas *et al.*,

478 2002, and Guillaume Martin for his help with identifying the equilibria of the mathematical
479 model. We also thank Bouwe Cattrysse for generating exploratory pilot data for the LonX-c
480 and LonX-w lines. NW was supported by a BOF post-doctoral fellowship (Ghent University,
481 01P03420) and by a Research Foundation - Flanders (FWO) Research Grant (1513719N).
482 This work was further supported by the FWO Research Network EVENET. This is contribution
483 ISEM-2023-125 of the Institute of Evolutionary Science of Montpellier (ISEM).

484 **Author contribution statement**

485 NW conceived and designed the experiments. NW, EVR, and JZ performed
486 the experiments. FZ extended the model and performed the simulations. NW, FZ, and DB
487 analyzed the data. NW wrote the manuscript with input from FZ and DB. All authors read and
488 approved the final version of the manuscript.

489 **Conflict of Interest**

490 The authors declare no conflicts of interest.

491 **Data archiving**

492 All raw data and R scripts are available at the Dryad repository.

493 **References**

- 494 Beckmann JF, Bonneau M, Chen H, Hochstrasser M, Poinso D, Merçot H, *et al.* (2019). The Toxin–
495 Antidote Model of Cytoplasmic Incompatibility: Genetics and Evolutionary Implications.
496 *Trends in Genetics* **35**: 175–185.
- 497 Beckmann JF, Ronau JA, Hochstrasser M (2017). A *Wolbachia* deubiquitylating enzyme induces
498 cytoplasmic incompatibility. *Nat Microbiol* **2**: 17007.
- 499 Beckmann JF, Van Vaerenberghe K, Akwa DE, Cooper BS (2021). A single mutation weakens
500 symbiont-induced reproductive manipulation through reductions in deubiquitylation
501 efficiency. *Proc Natl Acad Sci USA* **118**: e2113271118.
- 502 Bing X, Lu Y, Xia C, Xia X, Hong X (2020). Transcriptome of *Tetranychus urticae* embryos reveals
503 insights into *Wolbachia* -induced cytoplasmic incompatibility. *Insect Mol Biol* **29**: 193–204.
- 504 Brooks ME, Kristensen K, van Benthem KJ, Magnusson A, Berg CW, Nielsen A, *et al.* (2017). glmmTMB
505 balances speed and flexibility among packages for zero-inflated generalized linear mixed
506 modeling.
- 507 Cattel J, Nikolouli K, Andrieux T, Martinez J, Jiggins F, Charlat S, *et al.* (2018). Back and forth
508 *Wolbachia* transfers reveal efficient strains to control spotted wing drosophila populations (J
509 Beggs, Ed.). *J Appl Ecol* **55**: 2408–2418.
- 510 Crawley M (2007). *The R book*. John Wiley & Sons: Hoboken, NJ.
- 511 Cruz MA, Magalhães S, Sucena É, Zélé F (2021). *Wolbachia* and host intrinsic reproductive barriers
512 contribute additively to postmating isolation in spider mites. *Evolution* **75**: 2085–2101.
- 513 Egas M, Vala F, Breeuwer JAJ (Hans) (2002). On the evolution of cytoplasmic incompatibility in
514 haplodiploid species. *Evolution* **56**: 1101–1109.

- 515 Enders MM (1993). The effect of male size and operational sex ratio on male mating success in the
516 common spider mite, *Tetranychus urticae* Koch (Acari: Tetranychidae). *Animal Behaviour* **46**:
517 835–846.
- 518 Engelstädter J, Hurst GDD (2009). The Ecology and Evolution of Microbes that Manipulate Host
519 Reproduction. *Annu Rev Ecol Evol Syst* **40**: 127–149.
- 520 Feiertag-Koppen CCM, Pijnacker LP (1982). Development of the female germ cells and process of
521 internal fertilization in the two-spotted spider mite *Tetranychus urticae* koch (Acariformes :
522 Tetranychidae). *International Journal of Insect Morphology and Embryology* **11**: 271–284.
- 523 Fujii Y, Kageyama D, Hoshizaki S, Ishikawa H, Sasaki T (2001). Transfection of *Wolbachia* in
524 Lepidoptera: the feminizer of the adzuki bean borer *Ostrinia scapulalis* causes male killing in
525 the Mediterranean flour moth *Ephestia kuehniella*. *Proc R Soc Lond B* **268**: 855–859.
- 526 Gebiola M, Giorgini M, Kelly SE, Doremus MR, Ferree PM, Hunter MS (2017). Cytological analysis of
527 cytoplasmic incompatibility induced by *Cardinium* suggests convergent evolution with its
528 distant cousin *Wolbachia*. *Proc R Soc B* **284**: 20171433.
- 529 Gong J-T, Li Y, Li T-P, Liang Y, Hu L, Zhang D, *et al.* (2020). Stable Introduction of Plant-Virus-Inhibiting
530 *Wolbachia* into Planthoppers for Rice Protection. *Current Biology*: S0960982220313646.
- 531 Gotoh T, Noda H, Ito S (2007). *Cardinium* symbionts cause cytoplasmic incompatibility in spider
532 mites. *Heredity* **98**: 13–20.
- 533 Helle W (1967). Fertilization in the two-spotted spider mite (*Tetranychus urticae*: ACARI).
534 *Entomologia Experimentalis et Applicata* **10**: 103–110.
- 535 Helle W, Sabelis MW (1985). *Spider mites. Their biology, natural enemies, and control*. Elsevier:
536 Amsterdam.
- 537 Himler AG, Adachi-Hagimori T, Bergen JE, Kozuch A, Kelly SE, Tabashnik BE, *et al.* (2011). Rapid
538 Spread of a Bacterial Symbiont in an Invasive Whitefly Is Driven by Fitness Benefits and
539 Female Bias. *Science* **332**: 254–256.
- 540 Hoffmann AA, Turelli M, Harshman LG (1990). Factors affecting the distribution of cytoplasmic
541 incompatibility in *Drosophila simulans*. **126**: 933–948.
- 542 Hosokawa T, Koga R, Kikuchi Y, Meng X-Y, Fukatsu T (2010). *Wolbachia* as a bacteriocyte-associated
543 nutritional mutualist. *Proceedings of the National Academy of Sciences* **107**: 769–774.
- 544 Jones DR (2005). Plant Viruses Transmitted by Thrips. *Eur J Plant Pathol* **113**: 119–157.
- 545 Katlav A, Cook JM, Riegler M (2021). Egg size-mediated sex allocation and mating-regulated
546 reproductive investment in a haplodiploid thrips species (T Houslay, Ed.). *Funct Ecol* **35**: 485–
547 498.
- 548 Katlav A, Cook JM, Riegler M (2022). Common endosymbionts affect host fitness and sex allocation
549 via egg size provisioning. *Proc R Soc B* **289**: 20212582.
- 550 Katlav A, Nguyen DT, Cook JM, Riegler M (2021). Constrained sex allocation after mating in a
551 haplodiploid thrips species depends on maternal condition. *Evolution* **75**: 1525–1536.

- 552 Kaur R, Shropshire JD, Cross KL, Leigh B, Mansueto AJ, Stewart V, *et al.* (2021). Living in the
553 endosymbiotic world of *Wolbachia*: A centennial review. *Cell Host & Microbe* **29**: 879–893.
- 554 Kitajima EW, Rodrigues JCV, Freitas-Astua J (2010). An annotated list of ornamentals naturally found
555 infected by *Brevipalpus mite*-transmitted viruses. *Sci agric (Piracicaba, Braz)* **67**: 348–371.
- 556 Lenth R, Singmann H, Love J, Buerkner P, Herve M (2022). emmeans: estimated marginal means, aka
557 least-squares means. *R Package*.
- 558 LePage DP, Metcalf JA, Bordenstein SR, On J, Perlmutter JI, Shropshire JD, *et al.* (2017). Prophage WO
559 genes recapitulate and enhance *Wolbachia*-induced cytoplasmic incompatibility. *Nature* **543**:
560 243–247.
- 561 Li G, Zhang Z-Q (2018). Does size matter? Fecundity and longevity of spider mites (*Tetranychus*
562 *urticae*) in relation to mating and food availability. *saa* **23**: 1796.
- 563 Ma W-J, Schwander T (2017). Patterns and mechanisms in instances of endosymbiont-induced
564 parthenogenesis. *Journal of Evolutionary Biology* **30**: 868–888.
- 565 Macke E, Magalhães S, Do-Thi Khanh H, Frantz A, Facon B, Olivieri I (2012). Mating Modifies Female
566 Life History in a Haplodiploid Spider Mite. *The American Naturalist* **179**: E147–E162.
- 567 Macke E, Magalhães S, Khan HD-T, Luciano A, Frantz A, Facon B, *et al.* (2011). Sex allocation in
568 haplodiploids is mediated by egg size: evidence in the spider mite *Tetranychus urticae* Koch.
569 *Proc R Soc B* **278**: 1054–1063.
- 570 Mitchell R (1972). The sex ratio of the spider mite *Tetranychus urticae*. *Entomologia Experimentalis et*
571 *Applicata* **15**: 299–304.
- 572 Navas-Castillo J, Fiallo-Olivé E, Sánchez-Campos S (2011). Emerging Virus Diseases Transmitted by
573 Whiteflies. *Annu Rev Phytopathol* **49**: 219–248.
- 574 Overmeer W, Harrison R (1969). Notes on the control of the sex ratio in populations of the two-
575 spotted spider mite, *Tetranychus urticae* Koch (Acarina: Tetranychidae). *New Zealand*
576 *Journal of Science* **12**: 920–928.
- 577 Penz T, Schmitz-Esser S, Kelly SE, Cass BN, Müller A, Woyke T, *et al.* (2012). Comparative Genomics
578 Suggests an Independent Origin of Cytoplasmic Incompatibility in *Cardinium hertigii* (NA
579 Moran, Ed.). *PLoS Genet* **8**: e1003012.
- 580 Perrot-Minnot M-J, Cheval B, Migeon A, Navajas M (2002). Contrasting effects of *Wolbachia* on
581 cytoplasmic incompatibility and fecundity in the haplodiploid mite *Tetranychus urticae*:
582 Contrasting effects of *Wolbachia* in a haplodiploid mite. *Journal of Evolutionary Biology* **15**:
583 808–817.
- 584 Poinot D, Bourtzis K, Markakis G, Savakis C, Merçot H (1998). *Wolbachia* Transfer from *Drosophila*
585 *melanogaster* into *D. simulans*: Host Effect and Cytoplasmic Incompatibility Relationships.
586 *Genetics* **150**: 227–237.
- 587 Potter DA, Wrensch DL, Johnston DE (1976). Guarding, Aggressive Behavior, and Mating Success in
588 Male Two-Spotted Spider Mites. *Annals of the Entomological Society of America* **69**: 707–711.

- 589 R Core Team (2021). R: A language and environment for statistical computing. R Foundation for
590 Statistical Computing, Vienna, Austria. URL <http://www.R-project.org>.
- 591 Robertson NL, Carroll TW (1988). Virus-Like Particles and a Spider Mite Intimately Associated with a
592 New Disease of Barley. *Science* **240**: 1188–1190.
- 593 Ross PA, Turelli M, Hoffmann AA (2019). Evolutionary Ecology of *Wolbachia* Releases for Disease
594 Control. *Annu Rev Genet* **53**: 93–116.
- 595 Ross PA, Wiwatanaratnabutr I, Axford JK, White VL, Endersby-Harshman NM, Hoffmann AA (2017).
596 *Wolbachia* Infections in *Aedes aegypti* Differ Markedly in Their Response to Cyclical Heat
597 Stress (EA McGraw, Ed.). *PLoS Pathog* **13**: e1006006.
- 598 Shan H-W, Luan J-B, Liu Y-Q, Douglas AE, Liu S-S (2019). The inherited bacterial symbiont
599 *Hamiltonella* influences the sex ratio of an insect host. *Proc R Soc B* **286**: 20191677.
- 600 Shropshire JD, Leigh B, Bordenstein SR (2020). Symbiont-mediated cytoplasmic incompatibility: what
601 have we learned in 50 years? *eLife* **9**: e61989.
- 602 Takafuji A, Ishii T (1989). Inheritance of sex ratio in the Kanzawa spider mite, *Tetranychus kanzawai*
603 Kishida. *Population Ecology* **31**: 123–128.
- 604 Tanahashi M, Fukatsu T (2018). *Natsumushi* : Image measuring software for entomological studies:
605 Image measuring software for entomology. *Entomological Science* **21**: 347–360.
- 606 Turelli M (1994). Evolution of Incompatibility-inducing Microbes and Their Hosts. *Evolution* **48**: 1500–
607 1513.
- 608 Vala F, Breeuwer JAJ, Sabelis MW (2000). *Wolbachia* –induced ‘hybrid breakdown’ in the two–
609 spotted spider mite *Tetranychus urticae* Koch. *Proc R Soc Lond B* **267**: 1931–1937.
- 610 Vala F, Van Opijnen T, Breeuwer JAJ, Sabelis MW (2003). Genetic Conflicts over Sex Ratio: Mite–
611 Endosymbiont Interactions. *The American Naturalist* **161**: 254–266.
- 612 Vavre F, Dedeine F, Quillon M, Fouillet P, Fleury F, Boulétreau M (2001). Within-species diversity of
613 *Wolbachia*-induced cytoplasmic incompatibility in haplodiploid insects. *Evolution* **55**: 1710–
614 1714.
- 615 Vavre F, Fleury F, Varaldi J, Fouillet P, Bouleatreau M (2000). Evidence for female mortality in
616 *Wolbachia* -mediated cytoplasmic incompatibility in haplodiploid insects: Epidemiologic and
617 evolutionary consequences. *Evolution* **54**: 191–200.
- 618 Wang Y-B, Ren F-R, Yao Y-L, Sun X, Walling LL, Li N-N, *et al.* (2020). Intracellular symbionts drive sex
619 ratio in the whitefly by facilitating fertilization and provisioning of B vitamins. *ISME J* **14**:
620 2923–2935.
- 621 Weeks AR, Breeuwer JAJ (2001). *Wolbachia* –induced parthenogenesis in a genus of phytophagous
622 mites. *Proc R Soc Lond B* **268**: 2245–2251.
- 623 Weinert LA, Araujo-Jnr EV, Ahmed MZ, Welch JJ (2015). The incidence of bacterial endosymbionts in
624 terrestrial arthropods. *Proceedings of the Royal Society B: Biological Sciences* **282**: 20150249–
625 20150249.

626 Wybouw N, Mortier F, Bonte D (2022). Interacting host modifier systems control *Wolbachia* -induced
627 cytoplasmic incompatibility in a haplodiploid mite. *Evolution Letters* **6**: 255–265.

628 Zélé F, Santos I, Matos M, Weill M, Vavre F, Magalhães S (2020). Endosymbiont diversity in natural
629 populations of *Tetranychus* mites is rapidly lost under laboratory conditions. *Heredity* **124**:
630 603–617.

631

632 **Figure Legends**

633 **Figure 1. *Wolbachia* induce two distinct reproductive phenotypes in *Tetranychus* mites.**
634 As *Tetranychus* mites have a haplodiploid mode of reproduction, unfertilized eggs develop into
635 haploid males, while fertilized eggs generate diploid females (control, top left). *Wolbachia*-
636 mediated sex allocation distortion facilitates successful egg fertilization and subsequent female
637 development, biasing population sex ratios towards females. In CI crosses, fertilized eggs
638 suffer from higher mortality rates (Female Mortality CI, FM-CI), or a proportion of fertilized eggs
639 reach adulthood as adult males (Male Development CI, MD-CI). A single CI cross can lead to
640 a mixture of FM-CI and MD-CI. Here, CI strength varies across the illustrative CI crosses.

641

642 **Figure 2. *Wolbachia*-mediated sex allocation distortion is contingent on the host nuclear**
643 **genotype. Panel A:** Sex ratio from compatible within-line crosses for the infected and cured
644 lines of the Beis, LonX, and Stt host genotype. Sex ratio was calculated as the proportion of
645 females among the progeny that successfully reached adulthood. Host genotypes are ordered
646 according to decreasing CI strength. Statistical significance within each host genotype is
647 outlined above: *, $p < 0.05$, while ns, not significantly different at the 5% level. **Panel B:** Sex
648 ratio from compatible within-line crosses for the uninfected, infected, and cured line of the Stt
649 host genotype. Identical superscripts outline non-significant differences at the 5% level. For
650 both panels, boxplots and replicates are color coded based on the infection state (see bottom
651 middle). Each boxplot represents the 25%, 50%, and 75% quantile.

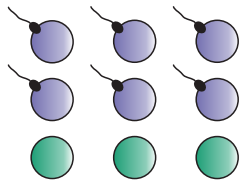
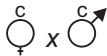
652 **Figure 3. Effects of *Wolbachia* infection on fecundity depend on the host nuclear**
653 **genotype.** Daily oviposition from fertilized females for the infected and cured lines of the Beis,
654 LonX, and Stt host genotype. Host genotypes are ordered according to decreasing CI strength.
655 Statistical significance within each host genotype is outlined above: *, $p < 0.05$, whereas ns,
656 not significantly different at the 5% level. Boxplots and replicates are color coded based on the
657 infection state (see bottom right). Each boxplot represents the 25%, 50%, and 75% quantile.

658 **Figure 4. *Wolbachia* distort sex allocation in *Tetranychus* mites by regulating egg**
659 **provisioning.** Egg size from fertilized females for the infected and cured lines of the Beis,
660 LonX, and Stt host nuclear genotype. Host genotypes are ordered according to decreasing CI
661 strength. Statistical significance within each host genotype is outlined above: *, $p < 0.05$,
662 whereas ns, not significantly different at the 5% level. Boxplots and replicates are color coded
663 based on the infection state (see bottom right). Each boxplot represents the 25%, 50%, and
664 75% quantile.

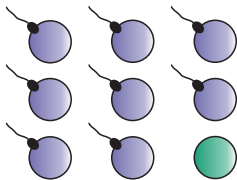
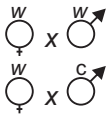
665 **Figure 5. *Wolbachia*-induced size difference can persist into the adult stage of**
666 ***Tetranychus* mites.** The projected body surface of teleiochrysalids as a proxy for adult size
667 for the infected and cured lines of the LonX and Stt host nuclear genotype (with males and
668 females in panel A and B, respectively). Statistical significance within each host genotype is
669 outlined above: *, $p < 0.05$, whereas ns, not significantly different at the 5% level. Boxplots and

670 replicates are color coded based on the infection state (see middle bottom). Each boxplot
671 represents the 25%, 50%, and 75% quantile.

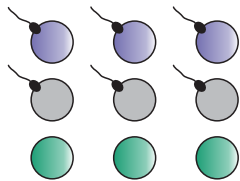
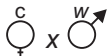
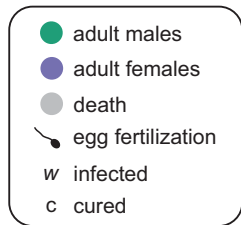
672 **Figure 6. Distortion of host sex allocation is expected to facilitate *Wolbachia* invasion.**
673 *Wolbachia* infection frequencies throughout host generations for initial infection frequencies
674 ranging from 0 to 1. Host genotypes are ordered according to decreasing CI strength. Dashed
675 red lines represent the unstable polymorphic equilibrium, which corresponds to ‘the threshold
676 infection frequency for *Wolbachia* invasion’. Blue lines represent the stable polymorphic
677 equilibrium, which is reached when the initial infection frequency is above the unstable
678 equilibrium. Our parametrized model does not predict a threshold infection frequency in Stt
679 despite a lower oviposition estimate upon *Wolbachia* infection. Additional simulations that
680 add/remove sex allocation distortion in Beis, LonX, and Stt further support the contribution of
681 sex allocation distortion to *Wolbachia* invasion (Figure S3).



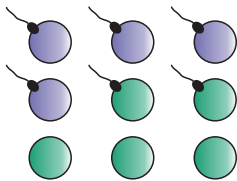
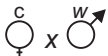
control



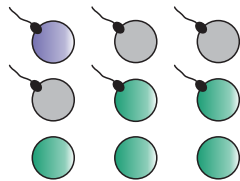
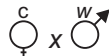
sex allocation distortion



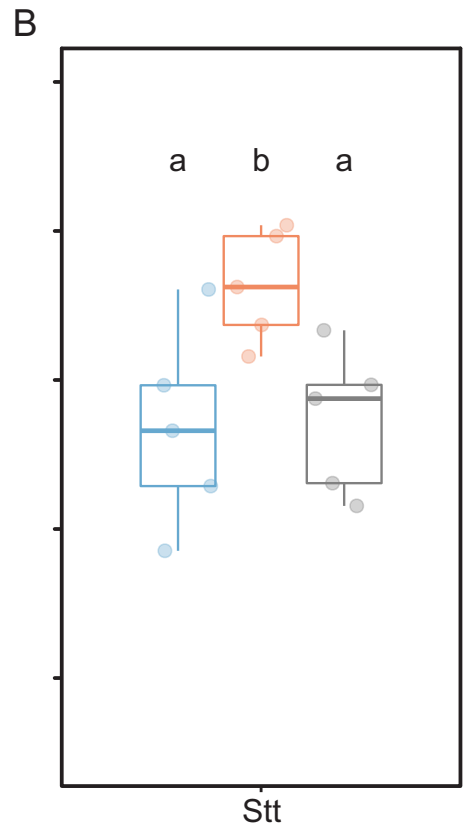
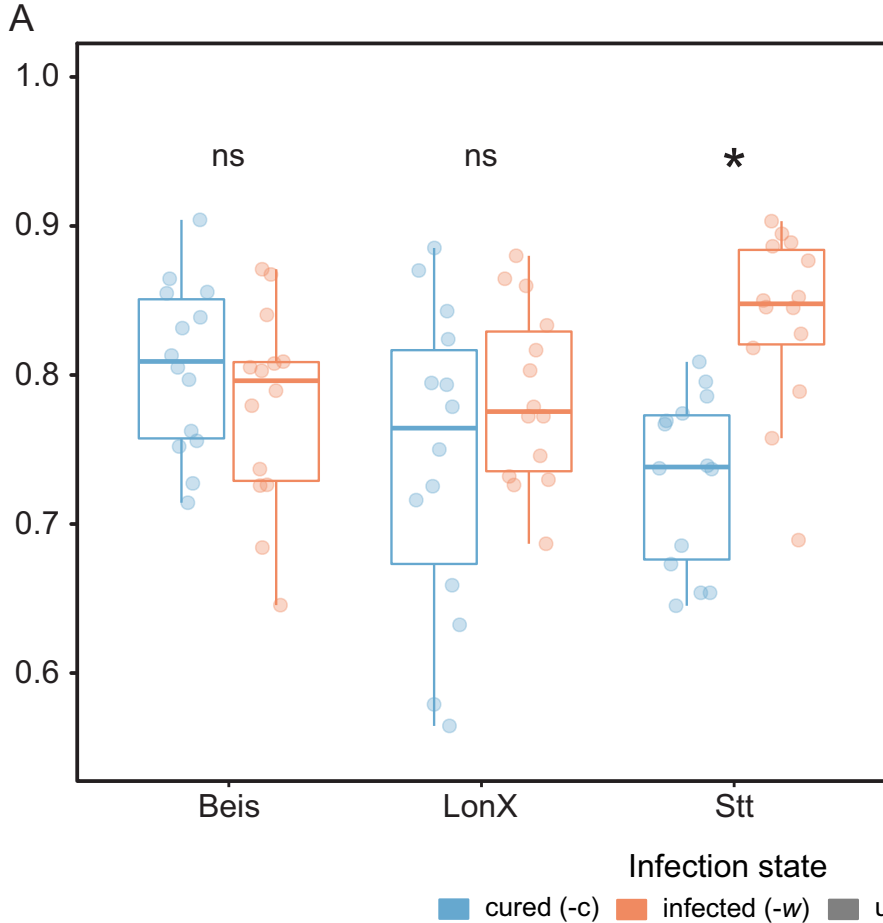
FM-CI



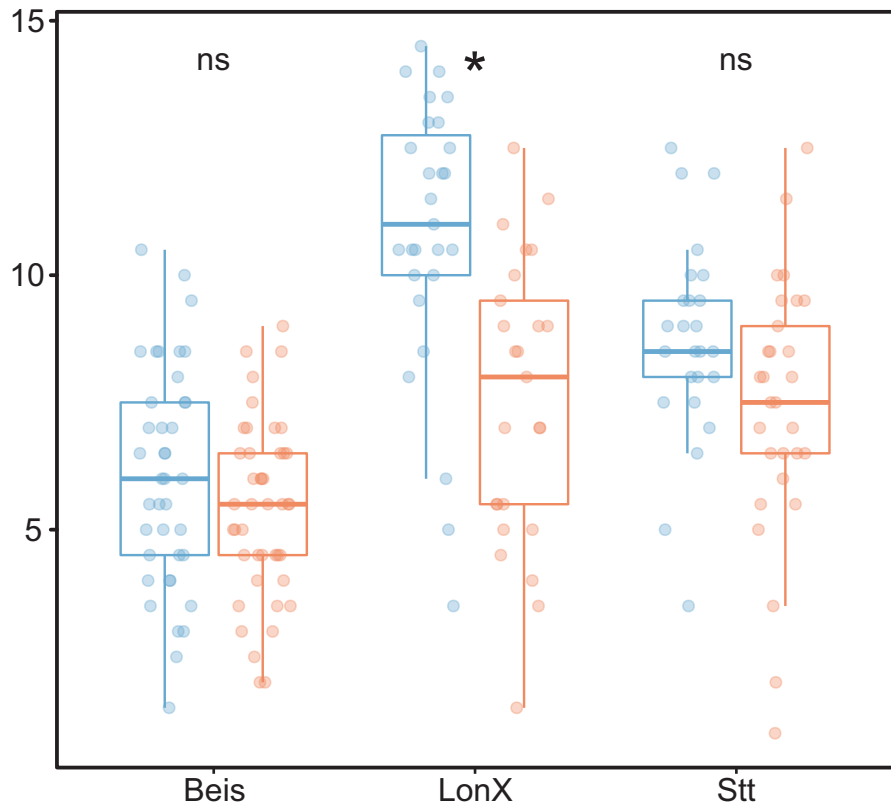
MD-CI



FM- and MD-CI



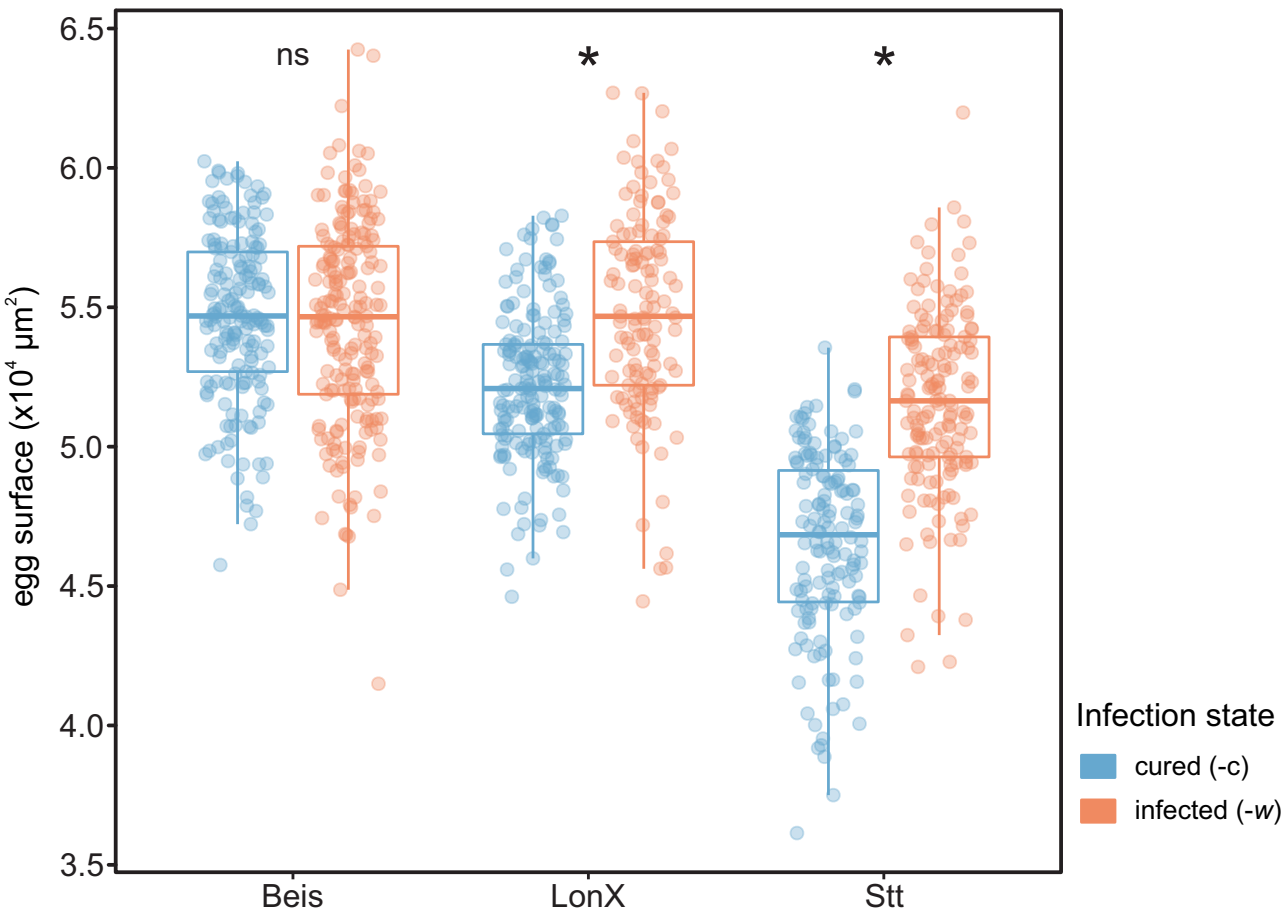
Daily oviposition per female



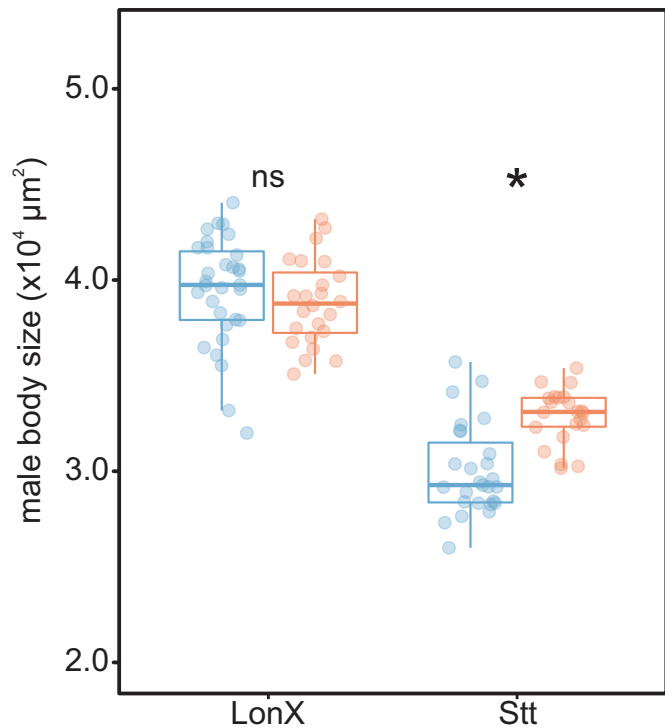
Infection state

cured (-c)

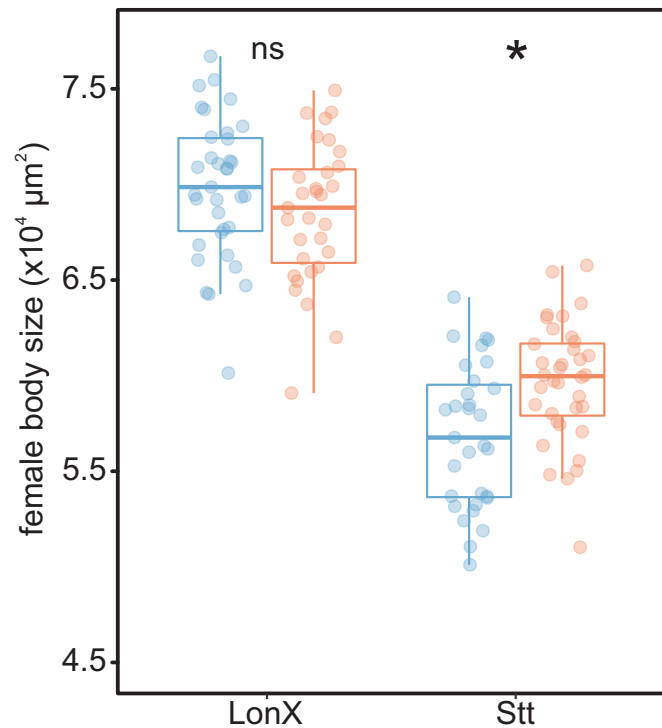
infected (-w)



A



B



Infection state

cured (-c) infected (-w)

